The 2012 World Congress on
Advances in Civil, Environmental, and Materials Research (ACEM' 12)
Seoul, Korea, August 26-30, 2012

An Electromechanically-Coupled Bernoulli-Euler Beam-Theory Taking into Account the Finite Conductivity of the Electrodes for Sensing and Actuation

*Juergen Schoeftner[1)] and Gerda Buchberger[2)]

[1)] *Institute of Technical Mechanics, Johannes Kepler University, Altenbergerstr. 69, 4040 Linz, Austria*
[1)] *juergen.schoeftner@jku.at*
[2)] *Institute for Microelectronics and Microsensors, Johannes Kepler University, Altenbergerstr. 69, 4040 Linz, Austria*
[2)] *gerda.buchberger@jku.at*

ABSTRACT

In this contribution an extended Bernoulli-Euler theory for a laminated beam is developed which takes into account elastic and piezoelectric material properties and resistive electrodes. The motivation of this study is to provide a deeper knowledge of the coupling mechanism of the mechanical and the electrical domain. This knowledge can be used to derive new strategies for active and passive vibration control and also for structural health monitoring of mechatronic systems. If the electrodes of a single piezoelectric layer are connected by an electrical resistance, the developed theory can be used for passive applications. Otherwise, if the voltage at a certain location of the electrode is controlled by a power supply, the presented theory also holds for actuated slender beams. The resulting coupled governing equations for the bending vibrations of the beam are (1) the well-known Bernoulli-Euler equation of a purely elastic beam, extended by a voltage term (forth order in space, second order in time), and (2) a diffusion equation for the voltage distribution (second order in space, first order in time) excited by the axial strain of the structure. In order to verify the derived extended beam theory, a slender beam is investigated and analytical results of the theory are compared to three-dimensional finite element results performed with ANSYS. Eigenfrequencies are compared for a clamped-free beam and different types of electrodes and electrical impedances (short and open circuits with either highly conductive or highly resistive electrodes). The frequency responses of the tip-displacement, the voltage distribution and the electrical field in the axial and in the thickness direction between analytical and FE results are in good agreement in the low and high frequency domain.

1. INTRODUCTION

Piezoelectric sensors and actuators have been widely used for the design of smart intelligent structures over the past decades. They might be bonded onto or embedded in a host structures. The use of piezoelectric transducers can be divided into three different fields: (i) the indirect piezoelectric effect is exploited to control the motion of a

[1)] Senior Scientist
[2)] Doctoral Candidate

system (actuation); (ii) the direct piezoelectric effect is used to observe the states of a system (sensor application, e.g. wave detection, structural health monitoring); and (iii) the vibration energy is converted into electrical energy (energy harvesting). For a review the reader is referred to (Mason 1981), (Chopra 2002) and (Crawley 1994).

In this contribution the focus of attention is set on piezoelectric transducers or patches, which are glued onto the surface of a slender beam-type structure. Mechanical models for the physical interaction of piezoelectric patches bond onto beams have been developed by (Crawley 1987) and (Chandra 1993). In (Krommer 2001) an electromechanically coupled beam theory within the framework of Bernoulli-Euler has been developed. This simple model, for which the governing equations of motion are similar to the Bernoulli-Euler equation of a purely elastic beam, is valid if either the total charge or the voltage over the electrodes is prescribed or if the charge density can be prescribed over the surface of the piezoelectric layers. The theory is validated by a two-dimensional plane stress calculation with Abaqus. An extension to the Timoshenko kinematic hypotheses is given in (Krommer 2002), where the developed theory is also compared to finite element results.

If no voltage supply is connected to the electrodes of the piezoelectric elements, the voltage is a function of the deformation. Such configurations are known as passive piezoelectric systems. Connecting the electrodes by resistances, inductances etc., a flexible structure is said to be passively controlled. The modeling of a passive moderately thick piezoelectric multimorph is presented by (Schoeftner 2011). The derived theory is an extension of the Timoshenko beam equations by means of a so-called non-local term, which describes the influence of the impedance of the attached electric circuit on the lateral motion of the beam. Based on this theory, the effect of the spatial distribution of the piezoelectric element is studied in (Schoeftner 2009) and (Schoeftner 2011b). It is shown that the concept of shape control can be also successfully applied to passive systems, and not only for an actuated piezo-beam: force-induced vibrations are completely annihilated along the beam axis for a specific target frequency if the shape of the electrodes and the inductive network are optimized.

All of the aforementioned references have in common that the electrodes of the piezoelectric elements are assumed perfect, i.e. the equipotential area condition is fulfilled over the electrode. A new arising field of interest is the use of piezoelectric layers with so-called resistive electrodes: it sounds curious, but from a control point of view, resistive or moderately conductive electrodes seem to be prospective candidates for active and passive vibration control. The distribution of the voltage can be controlled along the electrodes, in order to be most efficient, or the energy from structural vibrations is directly dissipated. So far, large area resistive electrodes are used as tactile sensors for touchpads (Buchberger 2008). To the best knowledge of the author, the only contribution dealing with the interaction of mechanical, electrical and piezoelectric properties is the work of (Lediaev 2010): a three-dimensional finite element formulation is set up which takes into consideration the presence of resistive electrodes. The frequency responses of the deformation and the potential and the eigenfrequencies are calculated for a cantilever bimorph with ideal, moderately conductive and hardly conductive electrodes.

The goal of this contribution is to develop a simple mechanical beam theory for laminated structures which is valid for both actuated and passive applications. The

resistance per unit length of the electrodes is included as a parameter in the derived equations and fully electromechanical coupling within our one-dimensional mechanical and electrical assumptions is considered. Finally our theory is validated by finite element calculation in ANSYS.

2. MODELLING OF A LAMINATED PIEZOELECTRIC BERNOULLI-EULER BEAM

The governing equation of a laminated slender beam (see the three-layer beam in Fig. 1a) within the kinematical assumption of Bernoulli-Euler, which consists of several elastic and/or piezoelectric layers $k = 1,...,N$ reads

$$M_w \ddot{w}_0 - M_{,xx} = q_z, \tag{1}$$

where w_0, M, q_z are the lateral displacement of the neutral axis, the bending moment and external distributed load. It is noted that these variables depend on the *x*-coordinate, i.e. the beam axis, and on the time *t*.

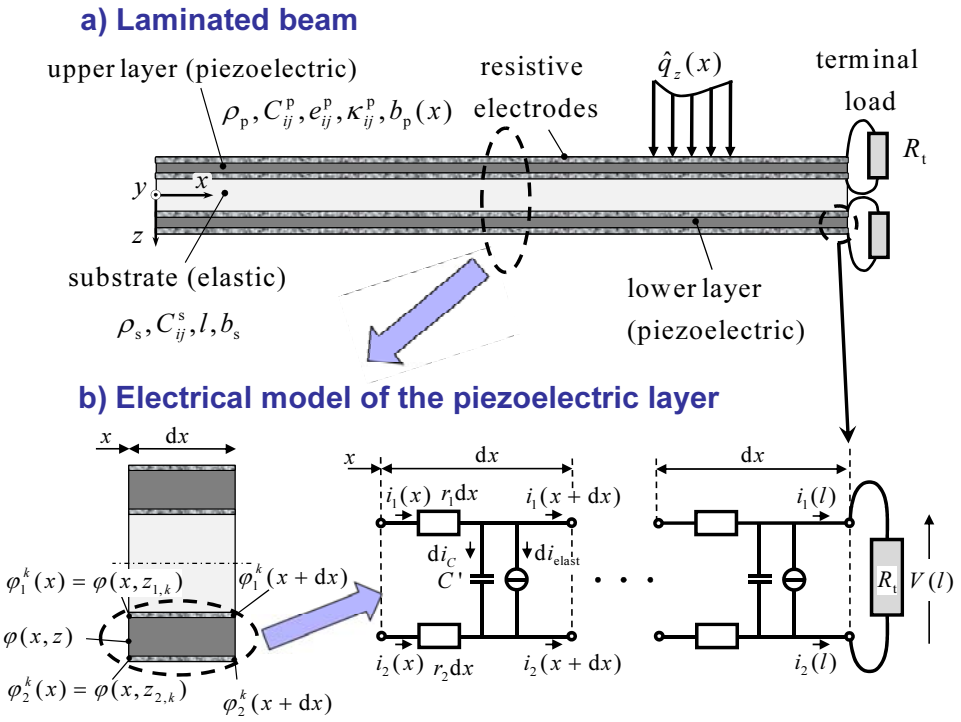

Fig. 1 a) Example of a three-layer beam (piezoelectric upper and lower layers, elastic middle layer), b) Block diagram of one piezoelectric layer with internal and external resistive electrodes

It is noted that in the following of this work the spatial derivatives with respect to *x* or *z* are written as

$$\frac{\partial f(x,z,t)}{\partial x} = f_{,x}(x,z,t) \qquad \frac{\partial f(x,z,t)}{\partial z} = f_{,z}(x,z,t). \tag{2}$$

The mass per unit length is defined by

$$M_w = \sum_{k=1}^{N} \int \rho_k b_k \left(z_{2k} - z_{1k} \right) \mathrm{d}x \tag{3}$$

where the density, the width of the layers and the thickness dimensions are given by $\rho_k, b_k, z_{2k}, z_{1k}$. The thickness of each layer is $h_k = z_{2k} - z_{1k}$. As it can be seen from Eq. (1), the differential equation for the lateral beam motion is a function of the bending moment distribution M of the beam. It is clear that this term depends on the deformation and the voltage. In order to find an appropriate expression, which includes both the direct and also the indirect piezoelectric effect, we first mention the linearized constitutive relations in Voigt notation for the axial stress

$$\sigma_{xx} = \tilde{C}_{11} \varepsilon_{xx} - \tilde{e}_{31} E_z . \tag{4}$$

The axial stress σ_{xx} is in general much higher than the remaining stress components $\sigma_{yy}, \sigma_{zz}, \sigma_{xy}, \sigma_{xz}, \sigma_{yz}$, see (Krommer 2001). The variables $\tilde{C}_{11}, \tilde{e}_{31}$ are the effective elastic and the piezoelectric modulus. Similar conclusions can be drawn for the mechanical strain ε_{xx}. The dominant direction of the electric displacement and the electric field are the thickness components D_z and E_z, for which the sensor equation reads

$$D_z = \tilde{e}_{31} \varepsilon_{xx} + \tilde{\kappa}_{33} E_z . \tag{5}$$

The strain-free permittivity is denoted as $\tilde{\kappa}_{33}$. Within the framework of the Bernoulli-Euler theory, which is a commonly used assumption when the thickness of the beam is rather small compared to the length, the axial strain is the negative product of the second derivative of the lateral displacement and the distance to the neutral beam axis

$$\varepsilon_{xx} = -z w_{0,xx}. \tag{6}$$

Often the electric field is often approximated as the quotient of the voltage drop and the thickness of the piezoelectric layer $E_z \approx V \big/ \left(z_2 - z_1 \right)$. As we will see later, this approximation is not exact in the sense, when bending deformations are taken into account, see Eq. (10). In order to find the potential distribution $\varphi_{,z}$, which is related to the electric field and the voltage drop V by

$$E_z(x,z,t) = -\varphi_{,z}(x,z,t) \qquad V\ (x,t) = \varphi_{,z}(x,z_2,t) - \varphi_{,z}(x,z_1,t), \tag{7}$$

we take advantage of Gauss' law of electrostatics. This reads, since the components D_x, D_y are neglected

$$D_{z,z} = 0. \tag{8}$$

Thus, D_z is constant along the thickness direction. Integration with respect to the thickness direction and taking advantage of (5), the electric displacement is found as a function of the displacement and the electric potential

$$D_z = \frac{1}{h}\int_{z_1}^{z_2} D_z \,\mathrm{d}z = -\tilde{e}_{31}\frac{\left(z_2 + z_1\right)}{2} w_{0,xx} - \frac{\tilde{\kappa}_{33}}{h} V. \tag{9}$$

Substituting Eq. (9) into (5), the following equation for the *z*-component of the electric field takes into account the influence of the bending deformation

$$E_z = -\frac{V}{h} + \frac{\tilde{e}_{31}}{\tilde{\kappa}_{33}}\left(z - z_m\right) w_{0,xx}. \tag{10}$$

Thus, it is shown that the bending deformation of the beam causes an electric field in the thickness direction. When comparing the eigenfrequencies of a piezoelectric bimorph in the case study (see section 5), the second term on the right-hand side of Eq. (10) causes additional stiffening (also see the analytical expression for the effective bending stiffness of the beam in Eq. (12), which includes the piezoelectric coefficient $\tilde{e}_{31}$).

The bending moment is calculated, when the electric field (10) is inserted into the axial stress equation (4) which is a function of $w_{0,xx}$ and V

$$M = \sum_{k=1}^{N}\int_{z_{1k}}^{z_{2k}} \sigma_{xx}^{k} b_k z \,\mathrm{d}z = -K_m w_{0,xx} + \sum_{k=1}^{N}\frac{\tilde{e}_{31}\left(z_{2k} + z_{1k}\right)}{2} b_k V^k. \tag{11}$$

The bending stiffness is defined by

$$K_m = \sum_{k=1}^{N}\tilde{C}_{11} b_k \frac{\left(z_{2k}^3 - z_{1k}^3\right)}{3} + \frac{\tilde{e}_{31}^{2k}\left(z_{2k} - z_{1k}\right)^3}{6\tilde{\kappa}_{33}^{k}}, \tag{12}$$

thus the extended version of the beam equation for a slender, laminated beam, consisting of *N* piezoelectric or elastic layers is derived from (11) and (1)

$$M_w \ddot{w}_0 + \left[K_m w_{0,xx}\right]_{,xx} = q_z + \left[\sum_{k=1}^{N}\frac{\tilde{e}_{31}\left(z_{2k} + z_{1k}\right)}{2} b_k V^k\right]_{,xx}. \tag{13}$$

The partial differential equation represents an extension of the well-known Bernoulli-Euler differential equation by means of the voltage-dependent term on the right-hand side. This equation is also denoted as actuator equation, since the trajectory of the lateral motion of the beam may be controlled by the voltage. For perfect electrodes, i.e. electrodes with infinite conductivity, the spatial derivation of the voltage with respect to *x* automatically vanishes and one finds the reduced form

$$M_w \ddot{w}_0 + \left[K_m w_{0,xx} \right]_{,xx} = q_z + \sum_{k=1}^{N} \frac{\tilde{e}_{31}\left(z_{2k} + z_{1k}\right)}{2} b_{k,xx} V^k \quad \text{(non-resisitive electrodes).} \tag{14}$$

Eq. (14) is in perfect agreement with the result from (Krommer 2001), when only perfect electrodes are considered, i.e. $V^k_{,x} = 0$. Since we are interested in the dynamics of piezoelastic beams with attached resistive electrode, the voltage distribution along the beam axis depends on the so-called resistance per unit length of the electrodes, i.e. $V^k_{,x} \neq 0$, see section 3.

It is noted that our beam theory also holds, if the axial dependency of the material parameters (e.g. $\tilde{C}_{11}, \tilde{e}_{31}, \tilde{\kappa}_{33}$) or the geometric dimensions (e.g. z_2, z_1, h_1) are functions of the beam axis *x*.

3. MODELLING OF THE VOLTAGE DISTRIBUTION OF RESISTIVE ELECTRODES

The block diagram of the piezoelectric layer and the surface electrodes (a reduced form of the telegraph equations) is shown in Fig. 1b. The resistance of the internal and external electrodes r_1, r_2 and the capacitance per unit length c of the piezoelectric layer are assumed to be piecewise constant functions in the *x*-direction. The index *1* stands for internal, and *2* for the external electrode. In the surrounding of *x*, the electrode currents i_1, i_2 are approximated by a Taylor series expansion

$$i_1(x + \mathrm{d}x) \approx i_1(x) + i_{1,x}(x)\mathrm{d}x \qquad i_2(x + \mathrm{d}x) \approx i_2(x) + i_{2,x}(x)\mathrm{d}x. \tag{15}$$

It is noted that these relations hold for each piezoelectric layer, but the index *k* and also the time-dependency *t* of the electrical variables is neglected for the sake of clarity. Next Kirchhoff's junction rule is applied, which states that at any node or junction in an electrical circuit, the sum of currents flowing into that node is equal to the sum of currents flowing out of that node

$$i_1(x + \mathrm{d}x) = i_1(x) - \mathrm{d}i_D(x) \qquad i_1(x + \mathrm{d}x) = i_1(x) + \mathrm{d}i_D(x). \tag{16}$$

The leakage current $\mathrm{d}i_D(x) = \mathrm{d}i_c(x) + \mathrm{d}i_{\mathrm{elast}}(x)$ flows through the piezoelectric layers and is equal to the time-derivation of the electric displacement multiplied by the infinitesimal small area $b(x)\mathrm{d}x$

$$\mathrm{d}i_D(x) = \dot{D}_z b(x)\mathrm{d}x \rightarrow i_{D,x}(x) = \dot{D}_z(x). \tag{17}$$

Substituting Eq. (9) into Eq. (17), and equating Eq. (15) with (16), one finds

$$\begin{aligned} i_{1,x}(x) &= -i_{D,x}(x) = \tilde{e}_{31}\frac{\left(z_2 + z_1\right)}{2} b\dot{w}_{0,xx} + \frac{\tilde{\kappa}_{33} b}{h}\dot{V} \\ i_{2,x}(x) &= i_{D,x}(x) = -\tilde{e}_{31}\frac{\left(z_2 + z_1\right)}{2} b\dot{w}_{0,xx} - \frac{\tilde{\kappa}_{33} b}{h}\dot{V} \qquad c = \frac{\tilde{\kappa}_{33} b}{h} \end{aligned} \tag{18}$$

Similarly, the potential over the internal and external electrode at location *x* is approximated by the Taylor series

$$\varphi_1(x+\mathrm{d}x) = \varphi_1(x) + \varphi_{1,x}\mathrm{d}x \qquad \varphi_2(x+\mathrm{d}x) = \varphi_2(x) + \varphi_{2,x}\mathrm{d}x. \tag{19}$$

Taking advantage of Kirchhoff's law, which states that the directed sum of the electrical potential differences around any closed network is zero, we find

$$\varphi_1(x+\mathrm{d}x) = \varphi_1(x) - i_1 r_1\,\mathrm{d}x \qquad \varphi_2(x+\mathrm{d}x) = \varphi_2(x) - i_2 r_2\,\mathrm{d}x. \tag{20}$$

Thus, equating Eq. (19) with Eq. (20), the voltage rule (in local form) for the resistive piezoelectric layer reads

$$-\varphi_{1,x} = i_1 r_1 \qquad -\varphi_{2,x} = i_2 r_2\,. \tag{21}$$

So the sensor equation, which is coupled to the actuator equation Eq. (13), describes the distribution of the voltage drop over the electrodes at any location *x*. It is obtained by subtracting both relations in Eq. (21), differentiating the result and using the Eq. (18) and the definition for the voltage drop at location *x* of the electrodes $V = \varphi_2 - \varphi_1$

$$V_{xx} = \varphi_{2,xx} - \varphi_{1,xx} = \frac{\tilde{\kappa}_{33} b}{h}\left(r_1 + r_2\right)\dot{V} + \tilde{e}_{31}\frac{\left(z_2 + z_1\right)}{2} b\left(r_1 + r_2\right)\dot{w}_{0,xx}. \tag{22}$$

4. EQUATIONS OF MOTION OF LAMINATED, PIEZOELECTRIC BEAM WITH RESISTIVE ELECTRODES

The governing equation for the lateral motion and the voltage distribution of a laminated slender beam with finitely conductive electrodes at the surfaces of the piezoelectric layers are given by the actuator and the sensor equation (Eqs. (13) and (22))

$$\begin{aligned} M_w \ddot{w}_0 + \left[K_m w_{0,xx}\right]_{,xx} &= q_z + \left[\sum_{k=1}^{N} \frac{\tilde{e}_{31}\left(z_{2k} + z_{1k}\right)}{2} b_k V^k\right]_{,xx} \\ V^k_{xx} &= \frac{\tilde{\kappa}^k_{33} b_k}{h_k}\left(r_1^k + r_2^k\right)\dot{V}^k + \tilde{e}^k_{31}\frac{\left(z_{2k} + z_{1k}\right)}{2} b_k \left(r_1^k + r_2^k\right)\dot{w}_{0,xx} \end{aligned} \tag{23}$$

It is noted that the sensor equation in Eq. (23) only holds for the lower piezoelectric layer of the bimorph. The voltage distribution for the upper layer is the same as for the lower layer, but the sign is reversed. Since the goal of this paper is to present a simple theory, we assume a very simple beam configuration:

- The beam is a bimorph with the *xy*-plane as a symmetry plane. Both layers are piezoelectric and the width of the beam is constant $b_k = \mathrm{const}$. Consequently, also the bending stiffness $K_m = \mathrm{const}$ and the mass per unit length $M_w = \mathrm{const}$ is also constant.

- The external force is uniformly distributed $q_z(x,t) = q_0(t)$

From the last simplification one concludes that due to the linearity of the differential equation it is advantageous to transform the differential equations into the frequency domain, e.g. by applying the Laplace transformation $L\{...\}$

$$L\{w_0(x,t)\} = \hat{w}_0(x,s),\ L\{V^k(x,t)\} = \hat{V}^k(x,s),\ L\{q_0(t)\} = \hat{q}_0(s). \tag{24}$$

The complex Laplace variable is denoted by s. Assuming that the initial conditions are zero, the beam equations (23) are transformed into the frequency-domain

$$\begin{aligned} s^2 M_w \hat{w}_0 + K_m \hat{w}_{0,xxxx} &= \hat{q}_0 + \tilde{e}_{31}\left(z_2 + z_1\right) b\ \hat{V}_{,xx} \\ \hat{V}_{,xx} &= \frac{\tilde{\kappa}_{33} b}{h}\left(r_1 + r_2\right) s\hat{V} + \tilde{e}_{31}\frac{\left(z_2 + z_1\right)}{2} b\ \left(r_1 + r_2\right) s\hat{w}_{0,xx}. \end{aligned} \tag{25}$$

The solution of (25) is given by

$$\begin{pmatrix} \hat{w}_0 \\ \hat{V} \end{pmatrix} = \sum_{j=1}^{6} \begin{pmatrix} \hat{w}_{0,j} \\ \hat{V}_j \end{pmatrix} e^{\lambda_j x} + \begin{pmatrix} \hat{q}_0 \\ 0 \end{pmatrix} \frac{1}{s^2 M_w}, \tag{26}$$

where the first part of the right-hand side fulfills the homogenous differential equation, whereas the second part is the inhomogeneous solution. The six eigenvalues $\lambda_1, ..., \lambda_6$ are obtained by find the roots of

$$\left(s^2 M_w + K_m \lambda_j^4\right)\left(\lambda_j^2 - \left(r_1 + r_2\right)\tilde{\kappa}_{33} b\ s / h\ \right) - \lambda_j^2 \tilde{e}_{31}^2 \left(z_2 + z_1\right)^2 b^2 \left(r_1 + r_2\right) s / 2 = 0. \tag{27}$$

The ratio of the amplitudes follows from one of the two equations in (25) and the homogenous part of the solution (26)

$$\frac{\hat{w}_{0,j}}{\hat{V}_j} = \frac{\tilde{e}_{31}\left(z_2 + z_1\right)\ b\ \lambda_j^2}{\left(s^2 M_w + K_m \lambda_j^4\right)} \text{ or } \frac{\hat{w}_{0,j}}{\hat{V}_j} = \frac{\lambda_j^2 - \left(r_1 + r_2\right)\tilde{\kappa}_{33} b\ s / h}{\tilde{e}_{31}\left(z_2 + z_1\right)\ b\ \lambda_j^2 \left(r_1 + r_2\right) s / 2}. \tag{28}$$

The 12 unknowns $\hat{w}_{0,1}, ... \hat{w}_{0,6}$ and $\hat{V}_1, ..., \hat{V}_6$ are determined if six boundary conditions (four mechanical and two electrical boundary conditions at $x = 0$ and $x = l$) are prescribed and Eq. (28) is taken into account.

5. NUMERICAL VALIDATION OF THE PRESENTED BEAM EQUATION BY MEANS OF THREE-DIMENSIONAL ELECTROMECHANICALLY COUPLED FINITE ELEMENT RESULTS

A figure of the piezoelectric cantilever bimorph is given in Fig. 2. At the right side the finite element model in ANSYS is shown. The thickness of each layer is $h = 5 \cdot 10^{-4}\,\mathrm{m}$, thus the total height of the beam is 0.001m. In order to model resistive electrodes, a resistor connects two neighboring nodes of the electrical degrees of freedom over the electrodes. The value of the resistance in the *x*- and the *y*-direction is the product of the

distance of two connected nodes and the resistance $R_x = r\Delta x$ and $R_y = r\Delta y$. The remaining parameters (material parameters and the geometry) of the two-layer structure are listed in Table 1.

Table 1 Numerical values for the bimorph in the case study

variable (unit)	value	variable (unit)	Value
$\rho\ \left(\mathrm{kgm^{-3}}\right)$	7750	$\tilde{C}_{11}\left(\mathrm{Nm^{-2}}\right)$	$6.15\cdot10^{10}$
$z_1\left(\mathrm{m}\right)$	0	$z_2\left(\mathrm{m}\right)$	$5.00\cdot10^{-4}$
$l\left(\mathrm{m}\right)$	0.04	$b\ \left(\mathrm{m}\right)$	$4.00\cdot10^{-3}$
$\tilde{\kappa}_{33}\left(\mathrm{AsV^{-1}m^{-1}}\right)$	$2.10\cdot10^{-8}$	$\tilde{e}_{31}\left(\mathrm{Asm^{-2}}\right)$	–10.483
$c\left(\mathrm{AsV^{-1}m^{-1}}\right)$	$1.68\cdot10^{-7}$	$q_0\left(\mathrm{Nm^{-1}}\right)$	25

In the following two subsections the eigenfrequencies and the harmonic response due to the spatial force loading q_0 of the displacement, the voltage distribution and the electric field are compared between our proposed extended beam theory and the results from the three-dimensional elasto-electrically coupled finite element simulation. For the piezoelastic layers the element SOLID5 is used, which takes into consideration the piezoelectric effect. For the resistor of the electrodes and the terminal load at the right side of the beam (see Fig. 2), the element CIRCU94 is used. The ANSYS model has 8 elements in the thickness, 4 elements in the lateral and 160 elements in the axial direction. A finer element mesh did not significantly change the result, but the computational time strongly increased.

5.1. Comparison of natural frequencies

The first three natural frequencies are listed in Table 2. Results are compared for a bimorph for which

- the piezoelectric effect is neglected: $\tilde{e}_{31}=0$
- ideal electrodes are assumed and internal and external electrodes are short-circuited: $r=0, R_t=0$
- ideal electrodes are assumed and internal and external electrodes remain unconnected: $r=0, R_t\to\infty$
- the electrodes are completely non-conductive: $r\to\infty$.

The order of the eigenfrequencies (i.e. the highest and lowest eigenfrequencies depending on the kind of electrodes and electric circuit) is the same for the finite element and for the analytical Bernoulli-Euler results, independent of the considered mode number. The highest frequencies obtained by the analytical results occur for the

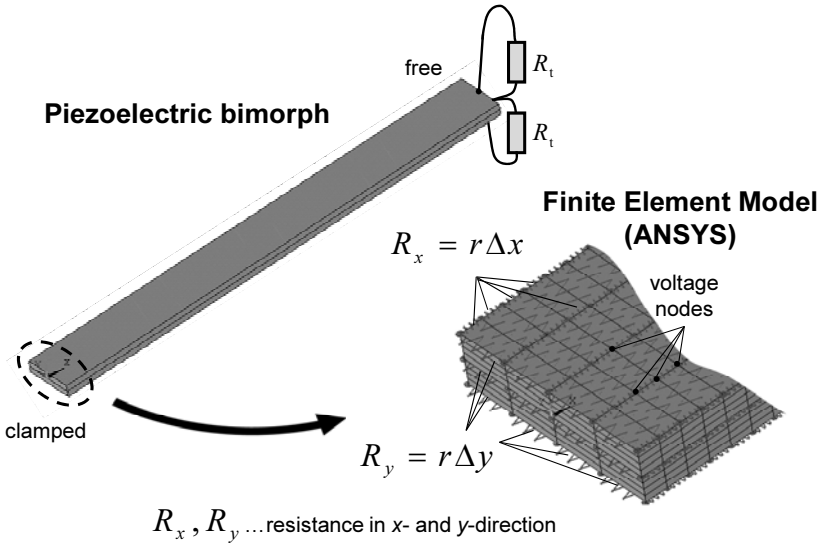

Fig. 2 Piezoelectric bimorph and the model of the resistive electrodes in ANSYS. Each voltage node of the internal and the external electrodes is connected via the resistors R_x, R_y to the adjoining voltage nodes

Table 2: Comparison of the bending eigenfrequencies of the bimorph cantilever between ANSYS(FE) and Bernoulli-Euler-beam (BE)

unit (Hz)	Bernoulli-Euler (analytical)			3d ANSYS		
electric circuit	f_1	f_3	f_3	f_1	f_2	f_3
elastic $\tilde{e}_{31}=0$	284.49	1782.9	4992.1	286.66	1791.3	4996.8
short circuit $r=0, R_t=0$	287.50	1801.7	5044.6	290.44	1814.8	5062.6
open circuit $r=0, R_t \to \infty$	292.83	1812.2	5055.0	295.87	1823.8	5073.8
non-electroded $r \to \infty$	296.27	1857.0	5199.8	299.76	1872.7	5224.5

non-electroded beam f_1=296.27Hz, followed by the open- and the short-circuited beam, f_1=292.83Hz and f_1=287.50Hz, respectively. If the piezoelectric effect is neglected, also the bending stiffness (see Eq. (12)) is the lowest and thus, the eigenfrequencies are the lowest f_1=284.49Hz. The results calculated by ANSYS are slightly higher, but the relative error is within 1% only. For the higher eigenfrequencies the quantitative agreement between analytical and numerical results is quite impressive: e.g. the third mode for the elastic beam occurs at f_3=4992.1Hz (BE) and f_3=4996.8Hz (ANSYS), the third natural frequencies with infinitely resistive electrodes are f_3=5199.8Hz (BE) and f_3=5224.5Hz (ANSYS).

It can be shown that the eigenfrequencies are also in good agreement for a simply-supported, a clamped-hinged and a clamped-clamped beam. These results are not listed in this contribution for the sake of clarity.

5.1. Comparison of the frequency response of electrical and mechanical variables

First, the results for the displacement along the beam axis and the potential distribution in the thickness direction of the beam are considered in the (quasi-)static frequency domain. Analytical results are plotted on the left side, Ansys results on the right side in Fig. 3-6.

The displacement $\hat{w}_0(x)$ is shown in Fig. 3. As expected from the eigenfrequency results, the non-electroded bimorph is the stiffest configuration. The tip deflection is only $0.359\mathrm{m}$ (BE) and $0.352\mathrm{mm}$ (ANSYS) respectively, and lower than all other configurations. The highest deflection occurs for the purely elastic beam, when the piezoelectric effect is neglected: $0.385\mathrm{mm}$ (BE) and $0.389\mathrm{mm}$ (ANSYS). The results for the open- and short circuited beams are between these results.

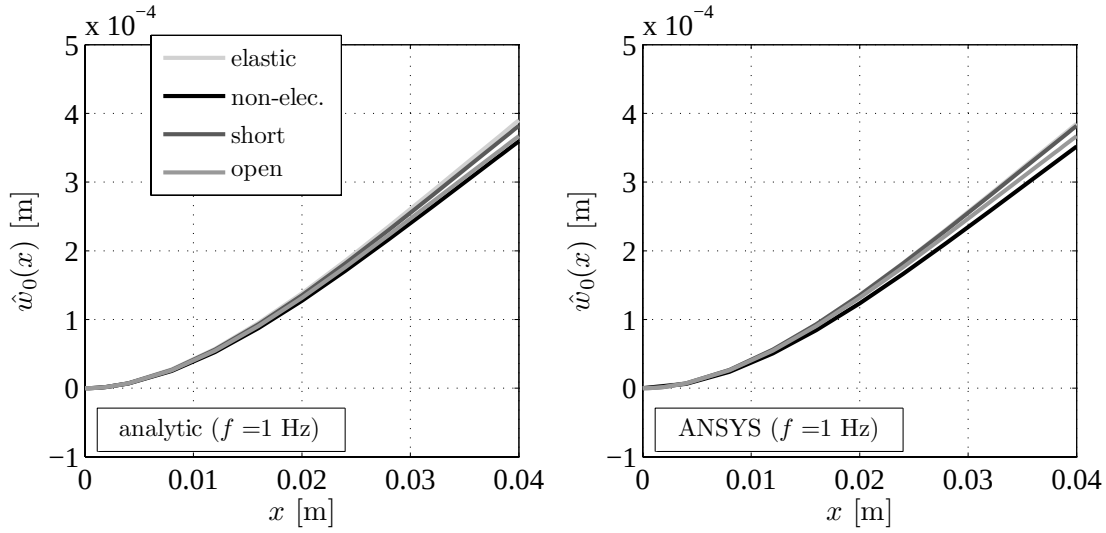

Fig. 3 (Quasi-)static deflection $\hat{w}_0(x)$ of the beam along the beam axis (excitation frequency *f*=1Hz)

In Fig. 4 one recognizes the voltage along the thickness of the beam $\hat{V}^*(0.5l,z) := \varphi(0.5l,z) - \varphi(0.5l,0)$. The middle axis of the beam is at $z = 0\mathrm{m}$ (neutral fibre) and the voltage of the external electrode of the lower layer is at $z = 0.0005\mathrm{m}$. As mentioned above, the voltage across the upper layer cross-section is the same, but opposite in sign. If ideal electrodes are assumed, which are kept at the same potential (short-circuit), one recognizes the quadratic distribution. This is a direct consequence of Gauss law of electrostatic and the assumption, that the electric field is the negative gradient of the potential, from which Eq. (10) follows: the electric field is a linear function of the second derivative of the displacement, thus the voltage is a quadratic function in *z*. It is noted that for slender beam structures, the lowest order

approximation for the electric field to be the quotient of the voltage and the thickness is not recommended by the authors, since the stiffness and the eigenfrequencies of the beam are underestimated and also Gauss law is not fulfilled. For the other electrical conditions under consideration, the voltage is a superposition of a linear and a quadratic part. When external and internal electrodes are not connected, but the equipotential area condition is satisfied, the voltage is $\hat{V}^*(0.5l, z_2) = 18.7\text{V}$ (BE) and $\hat{V}^*(0.5l, z_2) = 19.3\text{V}$ (ANSYS). In case of non-conductive electrodes $\hat{V}^*(0.5l, z_2) = 14\text{V}$ (BE) and $\hat{V}^*(0.5l, z_2) = 14.1\text{V}$ (ANSYS) holds.

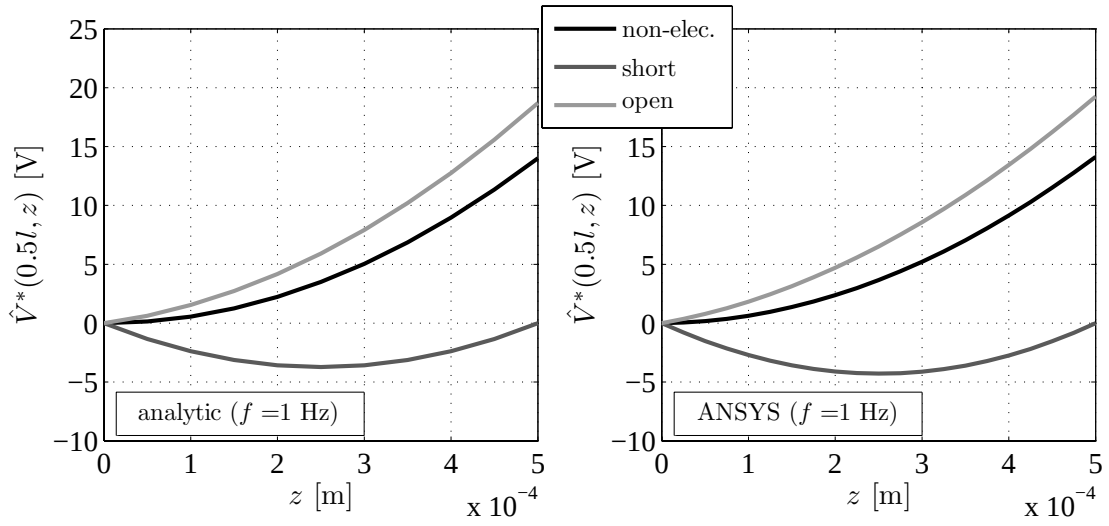

Fig. 4 (Quasi-)static voltage distribution in the thickness direction $\hat{V}^*(0.5l, z)$ (excitation frequency *f*=1Hz)

The results for the distribution of the electric field for the excitation frequency *f*=1500Hz (i.e. between the first and the second eigenfrequency, see Table 2) is shown in Fig. 5. Close to the clamped end, the ANSYS results show the influence of the mechanical boundary condition, which only have an effect in the close surrounding. For $x > 1\text{mm}$, these disturbances are negligible and the analytical results match the numerical ones very well. For the three electrode models, the maximum of the electric field is at location $x = 0.02\text{m}$ (e.g. open-circuit: $\hat{E}_z(0.5l, 0.6z_2) \approx 3.1 \cdot 10^4\,\text{V/m}$ (BE) and $\hat{E}_z(0.5l, 0.6z_2) \approx 2.9 \cdot 10^4\,\text{V/m}$ (ANSYS).

Finally, the frequency response of the tip displacement in the interval *f*=280-305Hz is shown. In the above part of the figure, results for the non-piezoelectric, the short- and open-circuited and the non-electroded beam are showns, whereas at the bottom the deflection curves of a bimorph with finite values for the resistance and the terminal load are drawn. One can reproduce the results for the eigenfrequencies, e.g. which read f_1=295.87Hz (open-circuit-ANSYS) and f_1=290.44Hz (short-ANSYS). As already mentioned, the main difference between analytical and numerical results is the frequency shift, which is approximately $\Delta f \approx 3\text{Hz}$. If the resistor of the electric circuit is

$R_t \approx 80.8\Omega$, the highest deflection is $\hat{w}_0(l) = 0.020\text{m}$ at *f*=293Hz (ANSYS), when the short- and open circuited curves intersect.

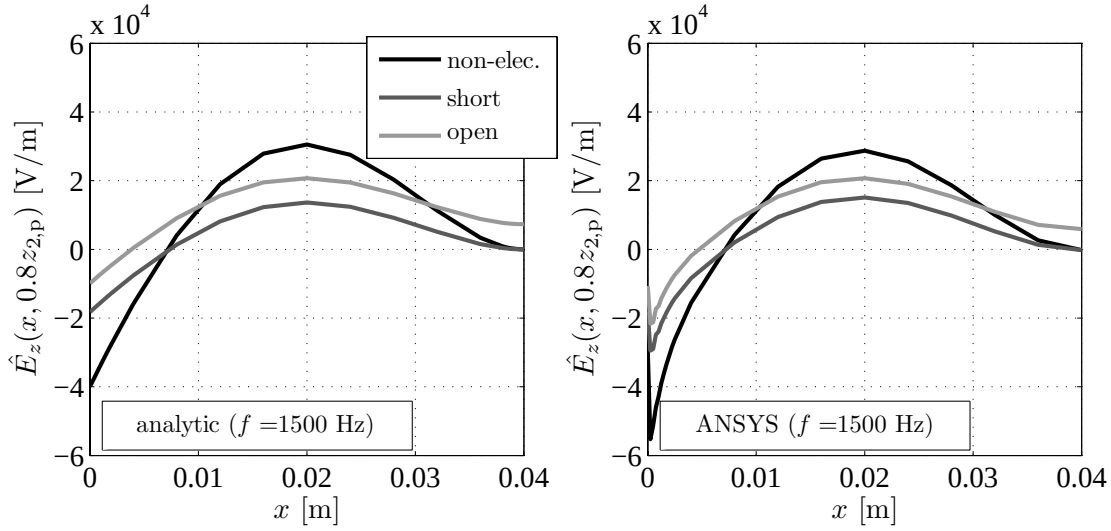

Fig. 5 Electric field $\hat{E}_z(x, 0.8z_2)$ along the beam axis (excitation frequency *f*=1500Hz)

Neglecting the circuit resistance $R_t \approx 0\Omega$ and choosing a resistance of $r \approx 2.6 \cdot 10^6 \Omega\text{m}^{-1}$, the maximal deflection is $\hat{w}_0(l) = 0.013\text{m}$ (ANSYS), which is the intersection point of deflection of the short- and the non-electroded bimorph. Open electrodes with a resistance $r \approx 9.7 \cdot 10^6 \Omega\text{m}^{-1}$ cause the highest deflection $\hat{w}_0(l) = 0.031\text{m}$ (ANSYS) of these simple damping strategies. It is obvious from the BE-results for the last three configurations that they are qualitatively similar to the ANSYS results.

CONCLUSION

In this contribution the governing equations of motion of a slender laminated piezoelectric beam with resistive electrodes have been presented. The Bernoulli-Euler kinematical assumptions have been assumed for the mechanical part, which have been combined with the one-dimensional constitutive relations of piezoelectricity, Gauss law of electrostatics and a reduced form of the telegraph equations for the resistive electrodes, in order to derive the actuation equation for the lateral beam motion and the sensor equation for the distribution of the voltage and the potential along the beam axis. It has been shown that for a piezoelectric beam with constant width and a uniformly distributed harmonic load, the mathematical effort to find a solution is comparable to one for a purely elastic beam.

The proposed theory has been compared to three-dimensional electromechanically coupled finite element simulations performed with ANSYS. The benchmark beam for the case study is a cantilever beam. Eigenfrequencies and the frequencies response of the displacement, the voltage and the electric field have not only been compared for

non-conductive, short- and open-circuited electrodes, but also when the internal and external electrodes are connected by an electric circuit and when a finite resistance per unit length is assumed.

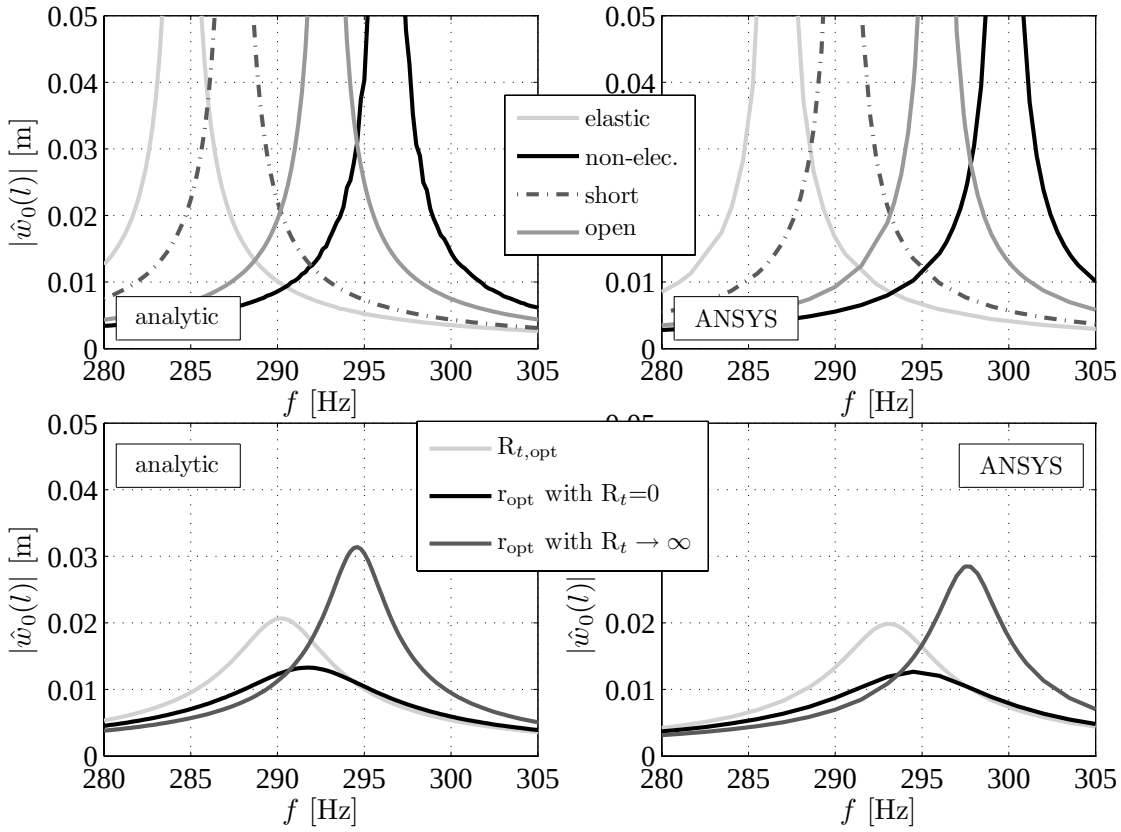

Fig. 6 Tip deflection $\hat{w}_0(l)$ between $f = 280 - 305\mathrm{Hz}$ (first bending eigenfrequency) for elastic, short-, open-circuited and non-electroded beam (above) and finite values for the resistance r and the terminal load R_t (bottom)

ACKNOWLEDGMENT

The research was funded by the COMET K2-Center ACCM and the Austrian Research Promotion Agency (FFG) under the contract number 825348/K-Licht.

REFERENCES

Mason, W.P. (1981) “Piezoelectricity, its history and applications”, *J. Acoust. Soc. Am.*, **70**, 1561-66.

Chopra, I. (2002) “Review of the state of art of smart structures and integrated systems”, *AIAA Journal*, **40**, 2145-87.

Crawley, E.F. (1994) “Intelligent structures for aerospace: a technology overview and assessment”, *AIAA Journal*, **32**, 689-99.

Chandra, R. and Chopra, I. (1993) “Structural modeling of composite beams with induced-strain actuators”, *AIAA Journal*, **31**, 1692-1701.

Crawley, E.F. and de Luis, J. (1987) “Use of piezoelectric actuators as elements of intelligent structures”, *AIAA Journal*, **25**, 1373-1385.

Krommer, M. (2001) “On the correction of the Bernoulli-Euler Beam theory for smart piezoelectric beams”, *Smart Mater. Struct*. **10**, 668-680.

Krommer, M. and Irschik, H. (2002) “An electromechanically coupled theory for piezoelastic beams taking into account the charge equation of electrostatics”, *Acta Mech*. **154**, 141-58.

Schoeftner, J. and Irschik, H. (2011), “A comparative study of smart passive piezoelectric structures interacting with electric networks: Timoshenko beam theory versus finite element plane stress calculations”, *Smart Mater. Struct.*, **20**, 025007 (13 pages).

Schoeftner, J. and Irschik, H. (2009), “Passive damping and exact annihilation of vibrations of beams using shaped piezoelectric layers and tuned inductive networks”, *Smart Mater. Struct.*, **18**, 125008 (9 pages).

Schoeftner, J. and Irschik, H. (20011b), “Passive shape control of force-induced harmonic lateral vibrations for laminated piezoelastic Bernoulli-Euler beams - theory and practical relevance”, *Smart Struct. Sys.*, **7**, 417-432.

Buchberger, G., Schwoediauer, R. and Bauer, S. (2008), “Flexible large area ferroelectret sensors for location sensitive touchpads”, *Appl. Phys. Lett.*, **92**, 123511 (3 pages)

Lediaev, L (2010), *Finite element modeling of piezoelectric bimorphs with conductive polymer electrodes*, Doctoral thesis Montana State University, Bozeman, Montana.